PLA-D-07-00688
09/11/07

Discrete moving breather collisions in a Klein-Gordon chain of oscillators

A Alvarez and FR Romero [1]

Grupo de Física No Lineal. Área de Física Teórica. Facultad de Física. Universidad de Sevilla. Avda. Reina Mercedes, s/n. 41012-Sevilla (Spain)

J Cuevas and JFR Archilla

Grupo de Física No Lineal. Departamento de Fisica Aplicada I. ETSI Informática. Universidad de Sevilla. Avda. Reina Mercedes, s/n. 41012-Sevilla (Spain)

Abstract

We study the collisions of moving breathers with the same frequency, traveling with opposite directions within a Klein-Gordon chain of oscillators. Two types of collisions have been analyzed: symmetric and non-symmetric, head-on collisions. For low enough frequency the outcome is strongly dependent of the dynamical states of the two colliding breathers just before the collision. For symmetric collisions, several results can be observed: breather generation, with the formation of a trapped breather and two new moving breathers; breather reflection; generation of two new moving breathers; and breather fusion bringing about a trapped breather. For non-symmetric collisions some possible results are: breather generation, with the formation of three new moving breathers; breather fusion, originating a new moving breather; breather trapping with breather reflection; generation of two new moving breathers; and two new moving breathers traveling as a bound state. Breather annihilation has never been observed.

Key words:
Discrete breathers, Moving breathers, Breather collisions, Klein-Gordon lattices
PACS: 63.20.Pw, 63.20.Ry, 63.50.+x, 66.90.+r, 87.10.+e

[1] Corresponding author. E-mail: romero@us.es

1 Introduction

The study of nonlinear localized excitations in lattices of oscillators, which receive the name of intrinsic localized modes or discrete breathers [1–4], is an active research field in nonlinear physics. These vibrational modes are rather generic in models of Klein-Gordon and FPU lattices [5–8]. They also appear as solutions of the Discrete Nonlinear Shrödinger (DNLS) equation [9] where these excitations are usually known as discrete solitons.

Under certain conditions, stationary breathers can be made mobile [10,11], i.e., when they experience appropriate perturbations, the breathers travel through the chain and they are called moving breathers (MBs). There are no exact solutions for MBs, but they can be obtained by means of numerical calculations. The conditions for the existence of MBs in Klein-Gordon lattices are strongly dependent on the exact details of both the on-site and the interaction potentials. One of the most thoroughly studied Klein-Gordon models where MBs appear is the Hamiltonian Klein-Gordon chain with Morse on-site potential and harmonic coupling potential [12–14]. Variants of this model have been proposed in the study of the DNA molecule, for example the Peyrard-Bishop model [15,16].

In a real discrete system, MBs should appear at arbitrary positions, then, it is natural to be interested in their collisions. The study of collisions of MBs has been initiated in FPU chains [17]. However, in Klein-Gordon chains, the studies have been limited to the interaction of moving low-amplitude breathers with stationary high-amplitude ones [18–20], or to the interaction between quasi-periodic moving breathers in dissipative lattices [21]. The study of soliton collisions in non-integrable DNLS models has not been undertaken until very recently. These models deal with nearly integrable DNLS equations [22,23], cubic DNLS equations [24] and saturable DNLS equations [25,26].

The aim of this paper is to get some insight into the detailed mechanisms and possible outcomes of collisions in a Klein-Gordon chain of oscillators with Morse on-site potential. We have considered only two types of collisions: a) symmetric collisions, that is, collisions of two identical MBs traveling with opposite velocities; b) non-symmetric collisions, or head-on collisions of two MBs with the same frequency but different velocities.

This article is organized as follows. Sec. 2 introduces the model, describes the means for producing MBs and different types of collisions. Sec. 3, presents the numerical simulations results corresponding to symmetric and non-symmetric head-on collisions. Sec. 4 presents some plausible explanations for the different outcomes. In Sec. 5, we compare the results for collisions of discrete solitons in DNLS models with the outcomes of our model. The summary and conclusions

are presented in Sec. 6.

2 Moving breathers and collisions

We consider a one-dimensional Klein-Gordon chain of identical oscillators. In scaled variables the Hamiltonian is given by:

$$H = \sum_n \left[\frac{1}{2}\dot{u}_n^2 + V(u_n) + \frac{1}{2}\varepsilon(u_n - u_{n+1})^2 \right], \tag{1}$$

where u_n represents the displacement of the nth oscillator from the equilibrium position, ε is the coupling parameter and $V(u_n)$ is the Morse on-site potential:

$$V(u_n) = \frac{1}{2}\left(\exp(-u_n) - 1\right)^2 . \tag{2}$$

Time-reversible, stationary breathers can be obtained using methods based on the anti-continuous limit[27]. At $t = 0$, $\dot{u}_n = 0, \forall n$, and the displacements of a breather centered at n_0 are denoted by $\{u_{SB,n}\}$. A moving breather $\{u_{t,n}\}$ can be obtained with the following initial displacements and velocities:

$$\begin{aligned} u^0_{MB,n} &= u_{SB,n}\cos(\alpha(n - n_0)) \\ \dot{u}^0_{MB,n} &= \pm u_{SB,n}\sin(\alpha(n - n_0)) \ . \end{aligned} \tag{3}$$

The plus-sign corresponds to a breather moving towards the positive direction and the minus one, the opposite. This procedure taken from the DNLS context [24,25] works as well as the marginal-mode method [10,11] and gives good mobility for a large range of ε. The parameter α is the difference of phase between two neighboring oscillators an we will refer to it as the *wave number*. The translational velocity and the translational kinetic energy of the MB increase with α. We use Eqs. (3) as initial conditions to integrate the dynamical equations using a symplectic algorithm [28]. The number of oscillators N is between 100 and 200 with periodic boundary conditions.

The study begins generating two MBs with the same frequency, located initially far apart, traveling in opposite directions. We have considered two different types of collisions, symmetric and non-symmetric collisions. For symmetric collisions, both MBs have initially the same displacements and opposite velocities given by Eqs. (3) with the same wave number α.

There are two types of symmetric collisions: a) on-site collisions (OS), if initially the centers of the breathers are separated by an odd number of particles, and b) inter-site collisions (IS), if that number is even [24,25].

3 Collision simulations

In this section, we present the results of the numerical simulations for symmetric and non-symmetric collisions. The breather frequency ω_b is below the phonon band because the on-site potential is soft. The lowest frequency of the phonon band is equal to the linear frequency of each isolated oscillator and is given by $\omega_0 = V''(0)^{1/2}$. For breathers with small amplitude the system is close to the linear limit, and their frequency is close to ω_0. Therefore, $|\omega_0 - \omega_b|$ is a measure of how far the system is from the linear regime. Hence, it is natural to think that the collision scenario should be strongly dependent of the common frequency of the two MBs. For that reason, we have considered two different breather frequencies, $\omega_b = 0.8$ and $\omega_b = 0.95$, that represent different degrees of nonlinearity. We describe below the different scenarios that appear considering the two types of collisions and the two frequencies.

Before considering collisions between MBs, it is necessary to have an estimate of their lifetime. A MB has not a single frequency but a continuous band around the frequency of the stationary breather. As this band contains phonon frequencies, phonons are excited and the breather loses energy. However, we have checked that in our system this energy is lost at a small rate and MBs propagate during several hundreds of periods without apparent decay (see Fig. 1). In our simulations, the time before the collision is something between 20 and 80 periods, therefore, we can consider that the colliding breathers are almost intact.

3.1 Symmetric collisions

We have performed an extensive study of collisions considering different values of the coupling parameter ε and MBs with different values of the wave number α. The values of ε have been taken in the interval [0.13,0.35] with step size 0.01. For each value of ε the values of α have been taken in the interval [0.030,0.200] with step size 0.002.

Generally, our simulations show that the outcome is strongly sensitive to the dynamical states of the MBs just before the collision.

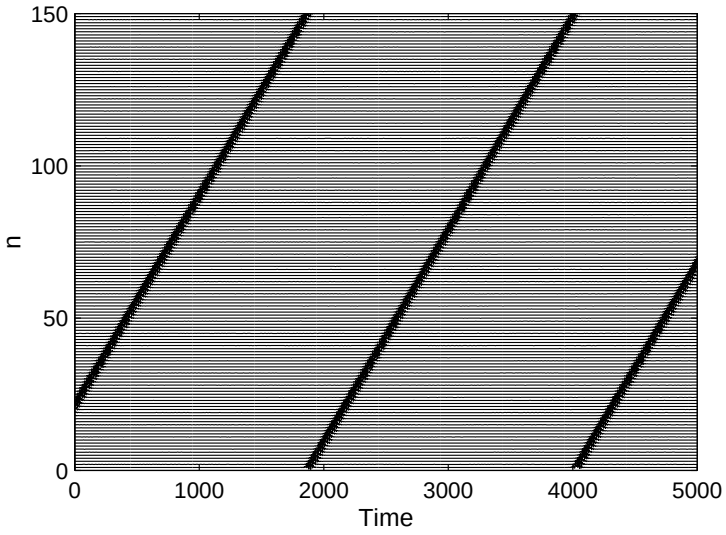

Fig. 1. Displacements versus time in a lattice with 150 oscillators. Wave number $\alpha = 0.1$; coupling parameter $\varepsilon = 0.32$ and breather frequency $\omega_{\rm b} = 0.8$

.

3.1.1 Symmetric collisions of breathers with frequency $\omega_{\rm b} = 0.8$

With this frequency and coupling parameter $\varepsilon = 0.32$, there are no significant differences between the outcomes of OS and IS collisions. The results can be summarized as follows:

(1) *Breather generation with trapping*:
The collision produces three new breathers, a trapped one located at the collision region, and two new symmetric MBs, as Fig. 2(a) shows for $\alpha = 0.048$. The trapped breather contains most of the initial energy. This behavior has been described in the pioneering work cited in Ref.[10].

Varying the parameter α, it is possible a noticeable attenuation of the amplitude of the trapped breather, which anticipates an entirely new outcome. Fig. 2(b) corresponds to $\alpha = 0.18$. In this case the emerging MBs contain most of the initial energy.

(2) *Breather reflection*:
With a slightly different value of α, it is possible a collision which results in two new symmetric MBs, with almost the same velocity that the colliding breathers'. This is shown in Fig. 2(c) for $\alpha = 0.19$.

The total energy transported by the colliding MBs is distributed after the collision: some part corresponds to the energy of the trapped breather, another part to the emerging MBs, and a small fraction of the energy is transferred to the lattice in the form of phonon radiation. In order to illustrate this phenomenon, we have studied the evolution of the "central energy", defined in our study as the energy of eleven particles around the collision region. This number of particles has been selected because it corresponds to the typical size

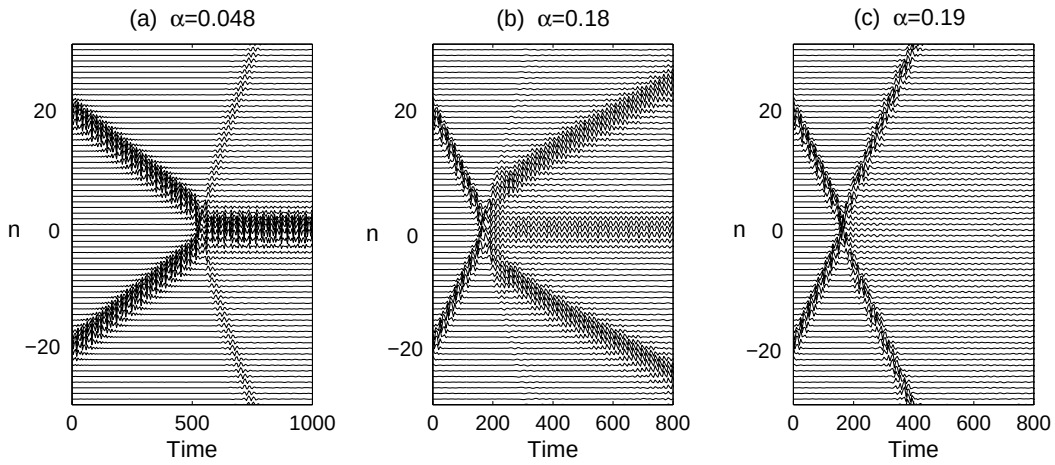

Fig. 2. Three examples of symmetric collisions with coupling parameter $\varepsilon = 0.32$ and frequency $\omega_{\rm b} = 0.8$. Displacements versus time for three different values of the wave number α: (a) $\alpha = 0.048$; (b) $\alpha = 0.18$; (c) $\alpha = 0.19$. Note that these behaviours occur in an apparently random way when α increases, although in these figures they seem to take place progressively.

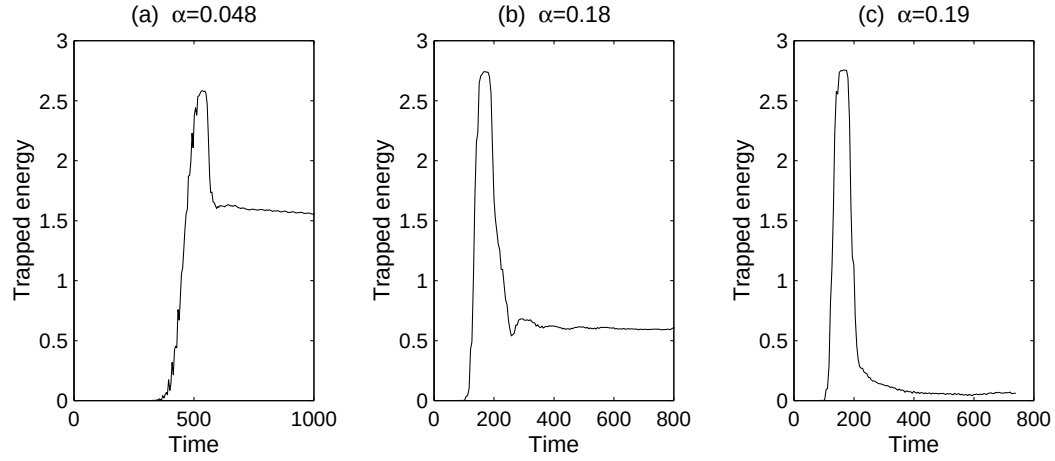

Fig. 3. Time evolution of the central energy corresponding to the collisions (a), (b) and (c) of Fig. 2, respectively.

of a discrete breather with the parameters used. Fig. 3 shows the evolution of the central energy for the three cases considered in Fig. 2.

Before the collision the central energy is zero; after the initiation of the collision it increases quickly, up to a value very close to the sum of the incident MBs energies; the subsequent decrease of the central energy is caused by the appearance of two emerging MBs and by phonon radiation.

The Fourier spectra of the breathers involved in the collisions of Fig. 2(a) are shown in Fig. 4. The trapped breather has a frequency ($\omega_{\rm trap} \sim 0.77$), which is lower than the colliding breathers', but its amplitude is larger. The

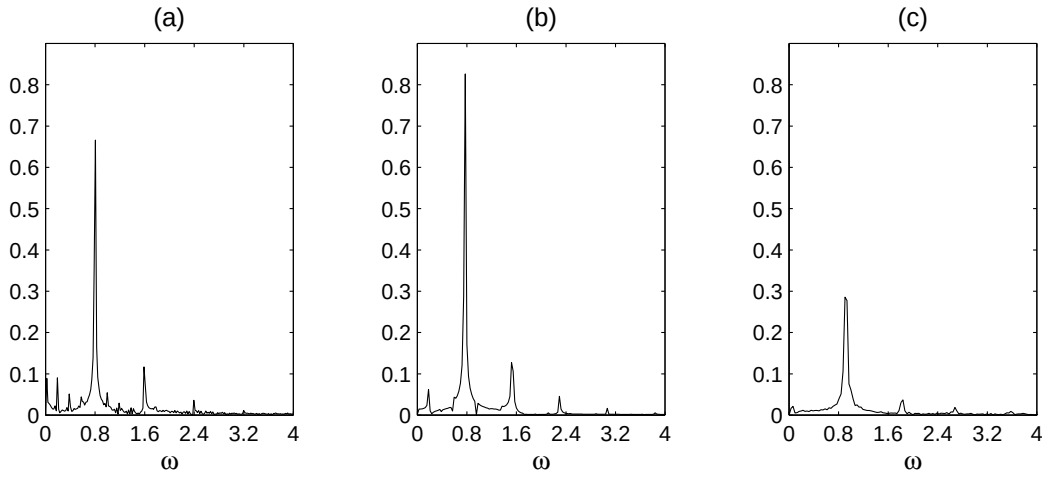

Fig. 4. Fourier spectra of the breathers involved in the collisions shown in Fig. 2(a). a) Incident breathers; b) trapped breather; c) emerging breathers.

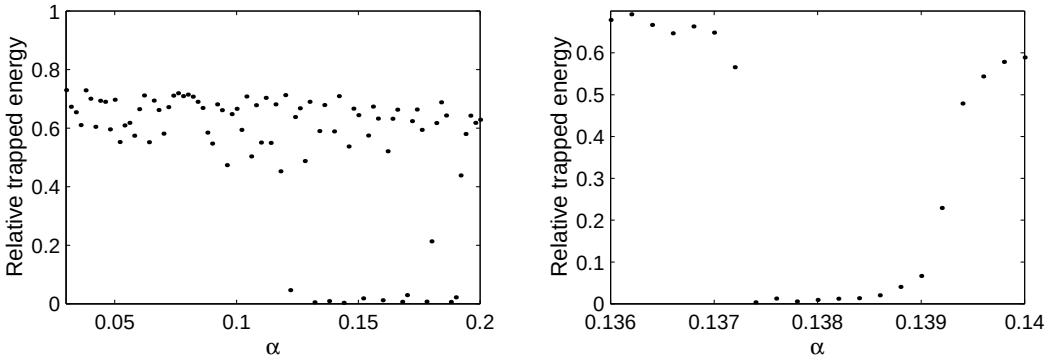

Fig. 5. (Left) Distribution of points representing the relative trapped energy versus wave number α, $\alpha \in [0.030, 0.200]$ with step size 0.002. Coupling parameter $\varepsilon = 0.32$; breather frequency $\omega_{\rm b} = 0.8$. (Right) Zoom around a value corresponding to breather reflection.

emerging MBs have higher frequency ($\omega_{\rm e} \sim 0.90$) and smaller amplitude than the colliding breathers'. We have also obtained the Fourier spectra for the breathers shown in Fig. 2(b) and (c). For the former, the trapped and emerging breathers have frequencies higher than the incident ones' ($\omega_{\rm trap} = 0.90$ and $\omega_{\rm e} = 0.86$, respectively), but smaller amplitudes. For the latter, the frequency of the reflected breathers is the same as the incident ones' indicating the quasi-elastic character of the scattering.

For each set of values (ε, α), we can calculate the relative trapped energy in the collision, defined as he ratio between the energy of the trapped breather and the sum of the energies of the two incident MBs. Taking $\varepsilon = 0.32$ and $\alpha \in [0.030, 0.200]$ with step size 0.002, we have obtained the relative trapped energies of these collisions which are represented by the distribution of points shown in Fig. 5 (left).

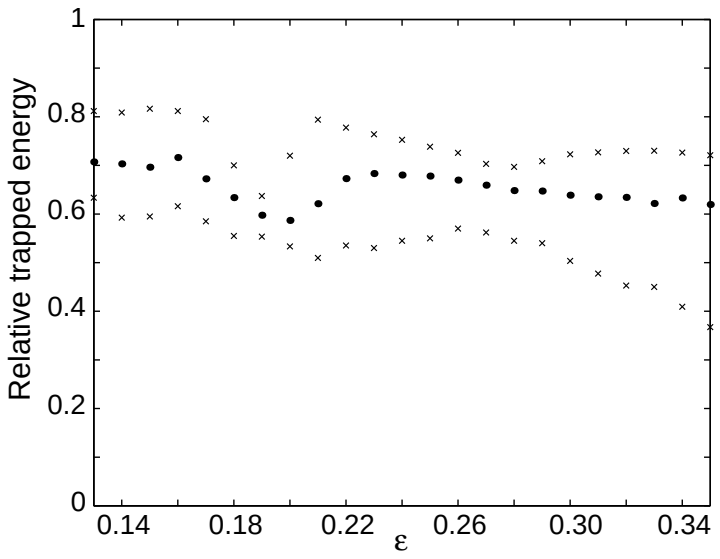

Fig. 6. Dots: dependence of the mean value of the relative trapped energies versus ε. Upper x-marks: dependence of the 98th percentile of the relative trapped energies versus ε. Lower x-marks: dependence of the 2nd percentile of the relative trapped energies versus ε.

Note that almost all points are distributed inside a band apparently at random. This means that a small change of α can affects the energy of the trapped breather. Occasionally, for large enough values of α, there are points outside the band which correspond to a relative trapped energy close to zero, i.e., for those values of α, the breathers are reflected. The behavior of the relative trapped energy around one of these points can be better appreciated if we choose a smaller step size for α. For example, if we take α within the interval [0.1360,0.1400] with step size 0.0002, we find that for $\alpha = 0.1370$ there is trapping, and for $\alpha = 0.1372$ the breathers are reflected. Fig. 5 (right) shows the behavior of the relative trapped energy around one of these values. There is an abrupt diminution of the relative trapped energy, that is, breathers reflection appears as an abrupt process for some exacts values of α.

Varying only the coupling parameter ε, we observe that the distributions of points are similar although the mean values of the relative trapped energies and the dispersion of points change. For each ε taken in the interval [0.13,0.35] with step size 0.01, we have obtained the corresponding distribution of points and we have calculated the mean value, the 98th and the 2nd percentile of the relative trapped energies. Fig. 6 shows the dependence of these quantities versus ε.

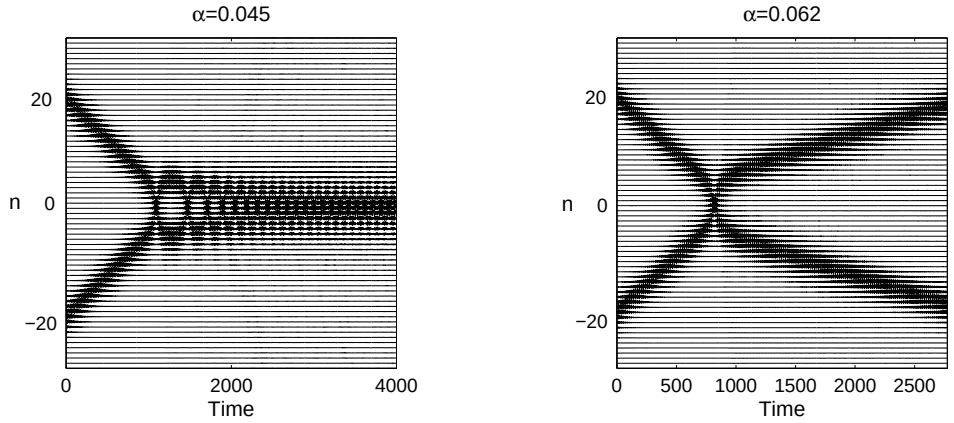

Fig. 7. Two examples of symmetric OS collisions with coupling parameter $\varepsilon = 0.32$ and breather frequency $\omega_{\rm b} = 0.95$. Displacements versus time for two different values of the wave number α. (Left) $\alpha = 0.045$. (Right) $\alpha = 0.062$.

3.1.2 Symmetric collisions of breathers with frequency $\omega_{\rm b} = 0.95$

For breather frequencies around this value, which is close to the frequency of an isolated oscillator in the linear regime, there are some important differences with respect to the previous case and there are only two possible outcomes.

(1) *Trapping*: For small enough incoming translational velocities, the outcome is a bound state of two trapped breathers whose distance oscillates with a decaying amplitude, i.e., the two trapped breathers have multiple rebounds, losing energy through phonon radiation and eventually decaying to a single stationary trapped breather.
(2) *Reflection*: There exists a critical value, α_c, of the wave number α, such that if $\alpha > \alpha_c$ the breathers are always reflected.

Fig. 7 shows these two outcomes for OS collisions with $\varepsilon = 0.32$ and $\omega_{\rm b} = 0.95$. The frequency of the trapped and reflected breathers of this figure are $\omega = 0.92$ and $\omega = 0.95$, respectively. The scenario for IS collisions is similar.

The critical value α_c depends on ε, and the simulations show that for low coupling, the values obtained with OS collisions are larger than for IS collisions. Nevertheless, they approach as ε increases and they are practically coincident for $\varepsilon > 0.22$. Fig. 8 shows the dependence of α_c versus ε for IS and OS collisions.

3.2 Non-symmetric collisions

The symmetry is broken if the incoming breathers have different translational kinetic energies. Clearly, in this case it is meaningless to distinguish between

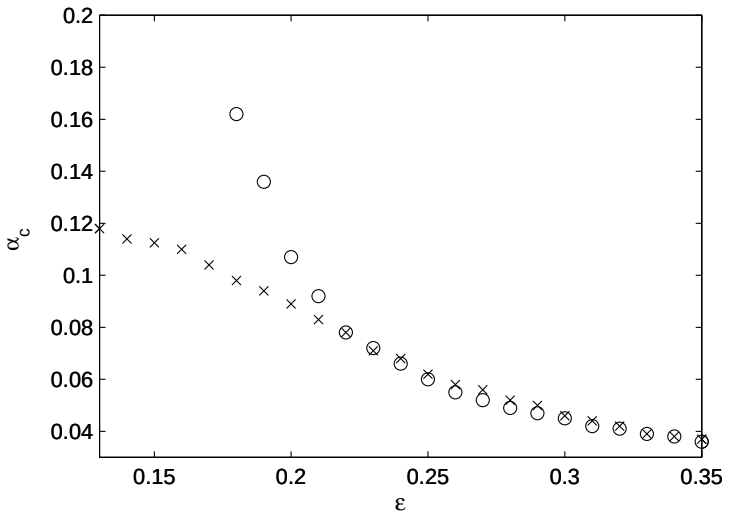

Fig. 8. Representation of the critical wave number α_c versus the coupling parameter ε for symmetric collisions of breathers with frequency $\omega_{\rm b} = 0.95$. Circles correspond to OS collisions and x-marks to IS collisions

OS and IS collisions due to the different breather velocities. The simulations show that there are many different outcomes, so we briefly describe some of them. Hereafter, the two MBs are denoted as MB_1 and MB_2, and their wave numbers are represented by α_1 and α_2, respectively.

(1) *Collisions of breathers with frequency* $\omega_{\rm b} = 0.8$

(a) *Small coupling*:

There are many different outcomes. The simulations selected to present this case correspond to $\epsilon = 0.15$, $\alpha_1 = 0.042$, and $\alpha_2 \in [0.031, 0.2]$ with step size 0.001.

(i) For $\alpha_2 < \alpha_1$, i.e., MB_1 moves faster than MB_2, we have observed two main behaviours: 1) only a slow MB emerges traveling in the direction of MB_2; 2) a breather is trapped at the collision region with or without the appearance of two outgoing MBs.

(ii) For $\alpha_2 > \alpha_1$, i.e., MB_2 moves faster than MB_1, we have observed three main behaviours: 1) two MBs of different amplitudes emerge with different velocities and opposite directions, or with the same direction of MB_2 (in this case, the phonons can help to the formation of a bound state, as shown in Fig. 9–left); 2) a single trapped breather and a single MB of small amplitude traveling in the direction of either MB_1 or MB_2 (see Fig 9–right); 3) a slow MB in the direction of MB_1, and two emerging MBs with smaller amplitudes.

(b) *Large coupling*:

For large coupling the behaviours are rather different. Taking $\varepsilon = 0.32$, we have found either two MBs traveling in opposite directions or a MB with two MBs of small amplitude traveling in opposite

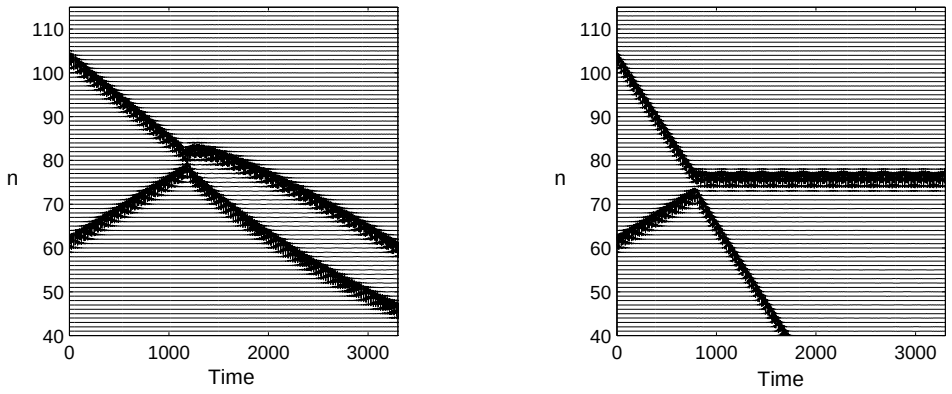

Fig. 9. Two examples of non-symmetric collisions with $\varepsilon = 0.15$, $\omega_b = 0.8$, and $\alpha_1 = 0.042$ with different outcomes. (Left) Two emerging MBs with the same direction, for $\alpha_2 = 0.061$. (Right) A reflected breather and the generation of a trapped breather, with $\alpha_2 = 0.131$.

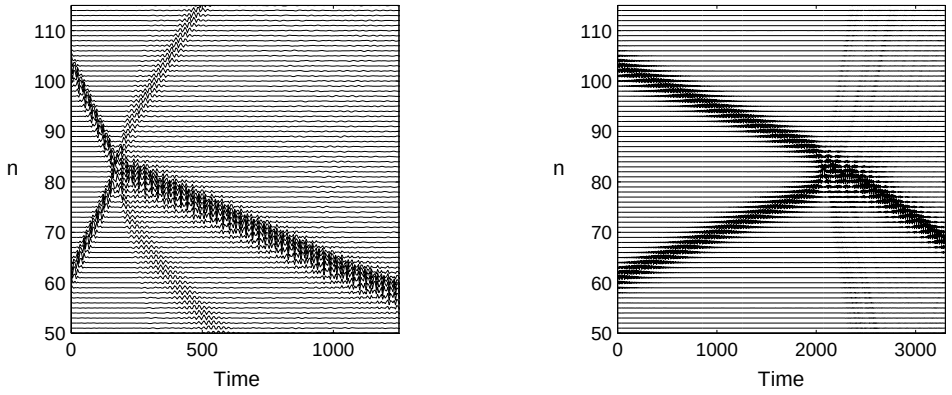

Fig. 10. (Left) A non-symmetric collision with the generation of three new MBs of different amplitudes, with $\varepsilon = 0.32$, $\omega_b = 0.8$, $\alpha_1 = 0.18$, and $\alpha_2 = 0.181$. (Right) Merging of two colliding MBs into a single MB, with $\omega_b = 0.95$, $\varepsilon = 0.14$, $\alpha_1 = 0.048$, and $\alpha_2 = 0.046$.

directions (see Fig. 10–left). We have not found any of the other results observed with low coupling.

(2) *Collisions of breathers with frequency* $\omega_b \sim 0.95$

If the breather frequency approaches to the bottom of the phonon band, i.e., the system is close to the linear regime, the asymmetric collisions almost always produce two reflected MBs. Nevertheless, at low coupling and small enough breathers velocities, the two MBs can merge originating a new MB. This occurs when the two MBs have almost the same velocities. Fig. 10–right illustrates a collision with $\omega_b = 0.95$, $\epsilon = 0.14$, $\alpha_1 = 0.048$ and $\alpha_2 = 0.046$.

4 Breather stability and trapping

There are some possible explanations for the trapping mechanism based in the stability properties of stationary breathers.

Consider a symmetric collision resulting in breather generation, as shown in Fig. 2 (a). The internal and kinetic energies of the breathers involved and the energy emitted through phonon radiation are related by

$$2U_{\rm in} + 2K_{\rm in} = U_{\rm trap} + 2U_{\rm out} + 2K_{\rm out} + U_{\rm ph}, \tag{4}$$

where $U_{\rm in}$ and $K_{\rm in}$ represent the internal and kinetic energies of each one of the incident breathers; $U_{\rm out}$ and $K_{\rm out}$ represent the internal and kinetic energies of each one of the emerging breathers; $U_{\rm trap}$ and $U_{\rm ph}$ represent, the internal energy of the trapped breather and the energy emitted through phonon radiation during the collision, respectively.

The on-site potential of our Klein-Gordon model is soft and, for this type of potential, an increase of the breather frequency corresponds to a decrease of the internal energy of the breather. The energy of the stationary breather versus $\omega_{\rm b}$, with $\epsilon = 0.32$, is shown in Fig. 11–(left). The frequency of a trapped breather is always different from the frequency of the incoming breathers, as the Fourier spectra shows. The generation of a trapped breather requires an amount of energy $U_{\rm trap}$, approximately equal to the energy of a stationary breather with the same frequency. Then, if the trapped breather has a frequency lower than the frequency of the incoming breathers, $U_{\rm trap} > U_{\rm in}$, and viceversa.

The sum of the internal and kinetic energies of a MB depends on α, ϵ and $\omega_{\rm b}$. Fig. 11–(right) shows the dependence of this sum with respect to α for MBs with $\epsilon = 0.32$ and $\omega_{\rm b} = 0.8$ (top), or $\omega_{\rm b} = 0.95$ (bottom).

Considering the collision shown in Fig. 2 (a), the frequencies of the trapped and emerging breathers are $\omega_{\rm trap} = 0.77$ and $\omega_{\rm e} = 0.90$, respectively. The following approximate results hold $2U_{\rm in} + 2K_{\rm in} = 2.6$, $2U_{\rm out} + 2K_{\rm out} = 1$, $U_{\rm trap} = 1.5$ and $U_{\rm ph} = 0.1$, which means that about 3.8% of the incident energy is lost as phonon radiation. However, for the collision shown in Fig. 7–left about 30% of the energy is lost as phonon radiation.

As we have shown, when two MBs collide, the excited region emits phonon radiation and the oscillators have a small frequency shift. For symmetric collisions, this shift depends on α, ϵ and $\omega_{\rm b}$. If a stationary breather with this new frequency is stable, a trapped breather appears and the remaining energy is emitted as two new MBs traveling with opposite directions (see Fig. 2 (a) , (b))

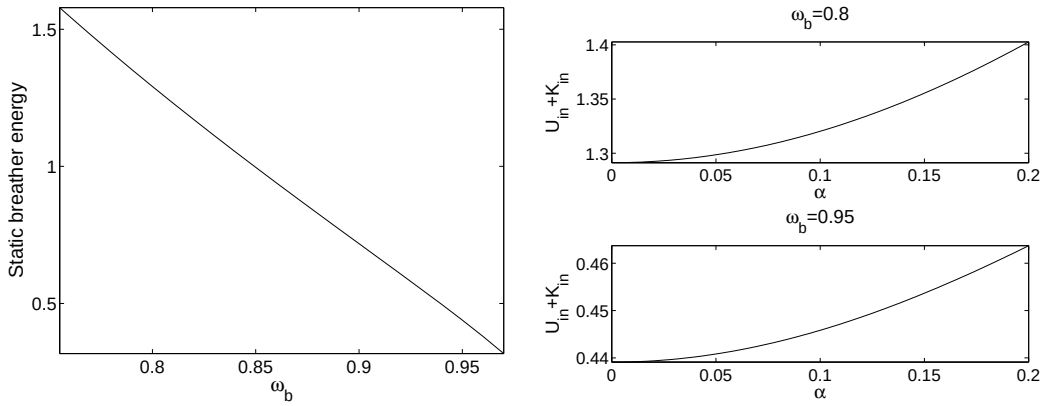

Fig. 11. (Left) Dependence of the energy of a stationary breather with respect to $\omega_{\rm b}$ with $\epsilon = 0.32$. The maximum value of the energy is $\tilde{E} = 1.5798$ and corresponds to $\omega_{\rm b} = \sqrt{0.25+\epsilon} = 0.7550$ (resonance of $2\omega_{\rm b}$ with the upper edge of the phonon band). (Right) Sum of the internal and kinetic energies versus α for breathers with $\epsilon = 0.32$ and $\omega_{\rm b} = 0.8$ (top), or $\omega_{\rm b} = 0.95$ (bottom).

or as additional phonon radiation (see the multiple rebounds in Fig. 7–left). However, if for the new frequency the stationary breather is unstable, there is no trapping at all and two new MBs appear traveling with opposite directions (see Fig. 2(c) and Fig. 7-right).

The stability of a breather can be studied by means of its Floquet eigenvalues. Considering a breather solution $\{u_n(t)\}$ with period T, if $\xi(t)$ and $\pi(t)$ represent a perturbation of the positions and velocities with respect to $\{u_n(t)\}$, the Floquet matrix $\mathcal{F}$ is defined as

$$\begin{bmatrix} \xi(T) \\ \pi(T) \end{bmatrix} = \mathcal{F} \begin{bmatrix} \xi(0) \\ \pi(0) \end{bmatrix} . \tag{5}$$

The Floquet matrix can be obtained by numerically integrating the perturbation equations:

$$\ddot{\xi}_n(t) + V''(u_n(t)) \cdot \xi_n(t) + \varepsilon(2\,\xi_n(t) - \xi_{n+1}(t) - \xi_{n-1}(t)) = 0\,. \tag{6}$$

The $2N$ eigenvalues of $\mathcal{F}$, $\{\lambda_i\}$, are called the Floquet multipliers. They can be expressed as $\lambda_i = \exp(\mathrm{i}\theta_i)$, where the complex numbers $\{\theta_i\}$ are called the Floquet arguments.

The perturbation equations are real and symplectic, which implies [6] that if λ_i is a multiplier, the complex conjugate λ_i^*, the inverse $1/\lambda_i$ and $1/\lambda_i^*$ are also multipliers. A perturbation parallel to $\dot{u}_n$ is also solution to the perturbation equations and it is called the *phase mode* because it represents a change in

the phase. As it is periodic, its multiplier has modulus 1 and, therefore, there is always a double 1 among the Floquet multipliers.

A breather is stable if every multiplier satisfy $|\lambda_i| \leq 1$, but if, for some i, $|\lambda_i| < 1$, then $|1/\lambda_i| > 1$. Therefore the stability condition is that every eigenvalue has modulus 1 (i.e., it belongs to the unit circle), or, equivalently, every Floquet argument is a real number.

If $\{u_n(t)\}$ corresponds to a stable breather with frequency $\omega_{\rm b}$, all the multipliers belong to the unit circle. If the frequency changes, the multipliers move along the circle, except the double 1 corresponding to the phase mode. The breather becomes unstable when the multipliers leave the circle and a stability bifurcation takes place. There are only three different bifurcation types:

a) Harmonic bifurcation: two multipliers coincide at 1 and leave the unit circle as real positive numbers, one smaller and the other larger than 1.

b) Subharmonic bifurcation: two multipliers coincide at -1 and leave the unit circle as real negative numbers, one smaller and the other larger than -1.

c) Oscillatory bifurcation: two complex eigenvalues collide and leave the unit circle as complex numbers (and their complex conjugates).

A further constraint for the appearance of a bifurcation is that the Krein signatures of the multipliers that are going to leave the unit circle must have different signs [6]. The Krein signature $\kappa(\lambda_i)$ of a complex multiplier λ_i with eigenvector $[\{\xi_n^i\}, \{\pi_n^i\}]$ is defined as:

$$\kappa(\lambda_i) = \text{sign}\left(\sum_n \text{i}\,[\xi_n^i(t)\pi_n^{i*}(t) - \xi_n^{i*}(t)\pi_n^i(t)]\right), \tag{7}$$

which does not change with time due to the symplectiness of Eqs. (6). The Krein signature $\kappa(\lambda_i)$ of a real multiplier is zero.

If $u_n = 0, \forall n$, the solutions of Eqs. (6) are the phonons given by $\xi_n^{\pm q} = \exp[\pm\text{i}\,(\omega_{\rm ph}(q)\,t - q\,n)]$ with frequencies $\omega_{\rm ph}(q) = [\omega_0^2 + 4\,\varepsilon\sin^2(q/2)]^{1/2}$ and wave numbers $q = 2\pi\,m/N$, $m = 0, \ldots, N-1$. The values of these solutions and their derivatives at $t = 0$, i.e., $[\{\xi_n^{\pm}(0)\}, \{\dot{\xi}_n^{\pm}(0)\}]$ are eigenvectors of the Floquet matrix, with multipliers $\lambda(\pm q) = \exp(\pm\text{i}\omega_{\rm ph}(q)\,T) = \exp(\pm\text{i}2\pi\omega_{\rm ph}(q)/\omega_{\rm b})$, arguments $\theta(\pm q) = \pm 2\pi\omega_{\rm ph}(q)/\omega_{\rm b} \pmod{2\pi}$, and Krein signatures $\kappa(\pm q) = \pm 1$. We will call them, for short, the *phonon multipliers* and *phonon arguments*.

If $\{u_n\}$ corresponds to a breather solution, most of the Floquet multipliers will be almost equal to the phonon ones, and more so, the larger the system. They will form two phonon bands within the unit circle, one with Floquet arguments

between $2\pi\omega_0/\omega_\mathrm{b}$ and $2\pi[\omega_0^2 + 4\,\varepsilon\sin^2(q/2)]^{1/2}/\omega_\mathrm{b}$ with Krein signature $+1$, and the corresponding complex conjugate band with Krein signature -1. For example, for $\varepsilon = 0.19$ and $\omega_\mathrm{b} = 0.8$, the phonon band "+" (with positive Krein signature) extends from 90° to 237°, the phonon band "-" extends from -90° to -237°. That is, the two phonon bands overlap and there are arguments with different Krein signature very close one to each other. Note that we have used in our simulations around 100 or 200 oscillators, therefore, there are nearly 100 or 200 Floquet arguments in each phonon band.

If ω_b changes, the phonons Floquet arguments move along the circle and many with different Krein signatures will cross, bringing about the possibility of instabilities. If we calculate numerically the Floquet arguments as a function of ω_b, we can observe that usually they leave the unit circle (i.e. the breather becomes unstable) and come back again inside it. There are very many frequency islands of instability and stability. Hence the extreme sensitivity of the outcome of the collision to the initial conditions. Moreover, not only the stability of the candidate to trapped breather changes but also the eigenvector corresponding to that instability and, as a consequence, the particular result of the non–trapping collision. At present we can not predict the small frequency shifts resulting of a symmetric collision, and therefore, its outcome.

5 Comparison with discrete soliton collisions in the DNLS equation

The scenarios for breather collisions in Klein-Gordon lattices can be compared with the scenarios for soliton collisions in non-integrable DNLS models. For these models, the known results deal with nearly integrable discretizations of the NLS equation [22,23], cubic DNLS equations [24] and saturable DNLS equations [25,26].

To start with, we consider the frequency $\omega_\mathrm{b} = 0.95$. For frequencies close to 1, breathers in Klein-Gordon lattices approximate to envelope discrete solitons of the DNLS equation (see e.g. [19,29,30]). Then, for the comparison we have selected the cubic DNLS equation [24], where a semi-analytical variational approximation correctly predicts the main features of the collisions.

For the cubic DNLS equation there exists a transmission and a merging regime for both OS and IS collisions (similar to our reflection and trapping regimes), and there is also a critical value for the wave number α that separates both regimes. Nevertheless, in the DNLS case there is a significant difference between the critical values for OS and IS collisions, which is explained by the existence of a high Peierls-Nabarro (PN) potential induced by the lattice. One of the most noteworthy phenomenon that appear for IS collisions is the possibility of bouncing after multiple collisions. For both types of collisions,

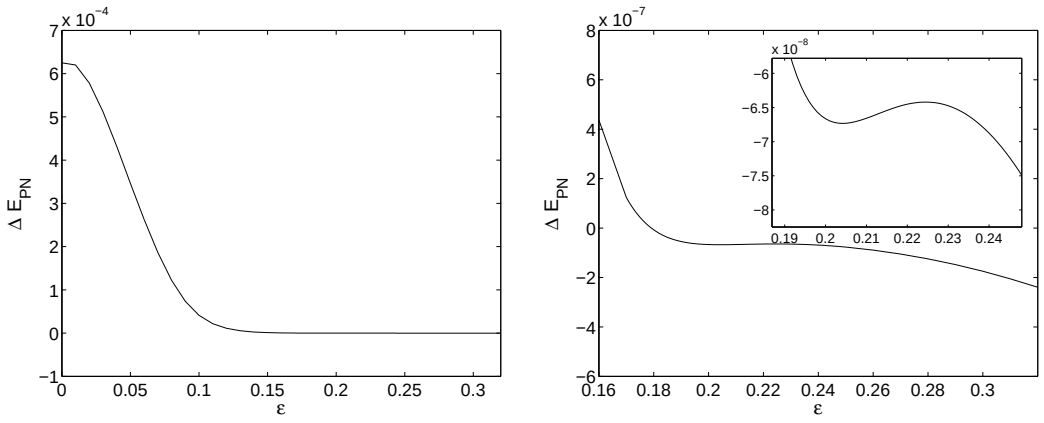

Fig. 12. (Left) Representation of the PN barrier versus the coupling parameter ε with breather frequency $\omega_{\rm b} = 0.95$. (Right) Two zooms of the left figure.

symmetry breaking is possible, its strongest manifestation being a merger of a pair of symmetric solitons into a single moving soliton.

The scenario in the Klein-Gordon chain is quite simple: we have neither found symmetry–breaking effects, nor bouncing after multiple collisions, and, contrary to the DNLS case, there is no qualitative differences between the OS and IS collisions. An explanation for this similitude can be found studying the PN barrier in our model. In Klein-Gordon lattices, the PN barrier has been defined as the difference between the energies of a two-site breather and a one-site breather, both with the same action [31]. Fig. 12–(left) shows the dependence of the PN barrier with respect to ε for $\omega_{\rm b} = 0.95$, note that the PN barrier is very small ($(\sim 10^{-7})$, which is the reason of the similitude between OS and IS collisions. There is a local minimum of the PN barrier in the interval $\varepsilon \in (0.20, 0.21)$, as Fig. 12–(right) shows.

Finally, we consider the frequency $\omega_{\rm b} = 0.8$. For the DNLS equations, there is no formation of bound states, there are only breather generation and breather reflection, and there is not a critical value of the wave number α separating these regimes. However, the DNLS equation with saturable nonlinearity [25,26] provides some similitudes, as there are reflection and generation regimes separated by a critical value of α. But in this DNLS case breather generation occurs only when α is larger than the critical value. The generation of bound states is also possible.

6 Conclusions

In this work, we have analyzed collisions of MBs in a Klein-Gordon model of oscillators. We have studied both symmetric and nonsymmetric head-on col-

lisions between breathers of the same frequency. We have considered different values of the coupling parameter, different velocities and different frequencies of the colliding MBs.

For symmetric collisions, we have found several scenarios: breather generation, with the formation of a trapped breather and two new moving breathers; breather reflection; generation of two new moving breathers; and breather fusion originating a trapped breather. For non-symmetric collisions the observed results are: breather generation, with the formation of three new moving breathers; breather fusion, originating a new moving breather; breather trapping with breather reflection; generation of two new moving breathers; and two new moving breathers traveling as a bound state. We have never observed breather annihilation.

For low enough frequency the outcome is strongly dependent of the velocities of the incident breathers and of their dynamical states when the collision begins. Very small changes of the velocities can determine an entire new outcome. This sensitivity disappears for frequencies close to the frequency of an isolated oscillator in the linear regime.

Some additional simulations are underway, these are: head-on collisions of two breathers with different frequencies and equal or different velocities; collisions of MBs with a stationary breather with equal or different frequencies; and collisions of two MBs traveling in the same direction with equal or different frequencies.

Acknowledgements

We acknowledge financial support from the MECD/FEDER project FIS2004-01183. We are also indebted to Panayotis G. Kevrekidis for his useful comments.

References

[1] Nonlinear Physics: Condensed Matter, Dynamical Systems and Biophysics - A Special Issue dedicated to Serge Aubry. *Physica D*, 216:1–246, 2006. Edited by T Dauxois, RS Mackay and GP Tsironis.

[2] Nonlinear localized modes: physics and applications. *Chaos*, 13:586–799, 2003. Focus issue edited by Yu S Kivshar and S Flach.

[3] Localization in nonlinear lattices. *Physica D*, 119:1–238, 1999. Focus issue edited by S Flach and RS Mackay.

[4] S Flach and CR Willis. Discrete breathers. *Phys. Rep.*, 295:181, 1998.

[5] RS MacKay and S Aubry. Proof of existence of breathers for time-reversible or Hamiltonian networks of weakly coupled oscillators. *Nonlinearity*, 7:1623, 1994.

[6] S Aubry. Breathers in nonlinear lattices: Existence, linear stability and quantization. *Physica D*, 103:201, 1997.

[7] AJ Sievers and S Takeno. Intrinsic localized modes in anharmonic crystals. *Phys. Rev. Lett.*, 61:970, 1988.

[8] J. Cuevas B. Sánchez-Rey, G. James and J.F.R. Archilla. Bright and dark breathers in Fermi-Pasta-Ulam lattices. *Phys. Rev. B*, 70:014301, 2004.

[9] K.Ø. Rasmussen P.G. Kevrekidis and A.R. Bishop. The Discrete Nonlinear Schrödinger equation. a survey of recent results. *Int. J. Mod. Phys. B*, 15:2833, 2001.

[10] Ding Chen, S Aubry, and GP Tsironis. Breather mobility in discrete ϕ^4 lattices. *Phys. Rev. Lett.*, 77:4776, 1996.

[11] S Aubry and T Cretegny. Mobility and reactivity of discrete breathers. *Physica D*, 119:34, 1998.

[12] J Cuevas, JFR Archilla, Yu B Gaididei, and FR Romero. Moving breathers in a DNA model with competing short- and long-range dispersive interactions. *Physica D*, 163:106, 2002.

[13] J Cuevas, F Palmero, JFR Archilla, and FR Romero. Moving breathers in a bent DNA model. *Phys. Lett. A*, 299:221, 2002.

[14] J Cuevas, F Palmero, JFR Archilla, and FR Romero. Moving discrete breathers in a Klein–Gordon chain with an impurity. *J. Phys. A: Math. and Gen.*, 35:10519, 2002.

[15] M Peyrard and AR Bishop. Statistical mechanics of a nonlinear model for DNA denaturation. *Phys. Rev. Lett.*, 62:2755, 1989.

[16] T Dauxois, M Peyrard, and CR Willis. Localized breather-like solution in a discrete Klein-Gordon model and application to DNA. *Physica D*, 57:267, 1992.

[17] Y. Doi. Energy exchange in collisions of intrinsic localized modes. *Phys. Rev. E*, 68:066608, 2003.

[18] T Dauxois and M Peyrard. Energy localization in nonlinear lattices. *Phys. Rev. Lett.*, 70:3935, 1993.

[19] K Forinash, M Peyrard, and BA Malomed. Interaction of discrete breathers with impurity modes. *Phys. Rev. E*, 49:3400, 1994.

[20] K Forinash, T Cretegny, and M Peyrard. Local modes and localization in a multicomponent nonlinear lattices. *Phys. Rev. E*, 55:4740, 1997.

[21] M. Meister and L.M. Floría. Bound states of breathers in the Frenkel-Kontorova model. *Eur. Phys. J. B*, 37:213, 2004.

[22] D. Cai, A.R. Bishop, and N. Gronbech-Jensen. Resonance in the collision of two discrete intrisic localized excitations. *Phys. Rev. E*, 56:7246, 1997.

[23] S.V. Dmitriev, P.G. Kevrekidis, B.A. Malomed, and D.J. Frantzeskakis. Two-soliton collisions in a near-integrable lattice system. *Phys. Rev. E*, 68:056603, 2003.

[24] I.E.
Papacharalampous, P.G. Kevrekidis, B.A. Malomed, and D.J. Frantzeskakis. Soliton collisions in the discrete nonlinear Schrödinger equation. *Phys. Rev. E*, 68:046604, 2003.

[25] J. Cuevas and J.C. Eilbeck. Discrete soliton collisions in a waveguide array with saturable nonlinearity. *Phys. Lett. A*, 358:15, 2006.

[26] A. Maluckov, L. Hadzievski, and M. Stepic. On symmetric breather collisions in lattices with saturable nonlinearity. *Eur.Phys.J.B*, 53:333, 2006.

[27] JL Marín and S Aubry. Breathers in nonlinear lattices: Numerical calculation from the anticontinuous limit. *Nonlinearity*, 9:1501, 1996.

[28] JM Sanz-Serna and MP Calvo. *Numerical Hamiltonian problems*. Chapman and Hall, 1994.

[29] O Bang and M Peyrard. Higher order breathers solutions to a discrete nonlinear Klein-Gordon model. *Physica D*, 81:9, 1995.

[30] AM Morgante, M Johannson, G Kopidakis, and S Aubry. Standing waves instabilities in a chain of nonlinear coupled oscillators. *Physica D*, 162:53, 2002.

[31] JA Sepulchre. Energy barriers in coupled oscillators: from discrete kinks to discrete breathers. In *Localization and Energy Transfer in Nonlinear Systems*, Singapore, 2003. World Scientific.